
sampe
Conference & Exhibition
May 20-23, 2019
CHARLOTTE, NC

sampe
Conference & Exhibition

75 years
INSPIRING PROFESSIONALS

Fiber Tow Deformations during layup of Steered Paths using Automated Fiber Placement Process

Roudy Wehbe, Brian Tatting, Zafer Gürdal, Ramy Harik
McNair Center, University of South Carolina

Outline

I. Introduction
   A. Introduction To AFP
   B. Tow Deformations Due To Steering
II. Problem Formulation
   A. Governing Equations
   B. Numerical Solution Approach
III. Results
   A. Steering Boundary Conditions
   B. Results For a Combined Tension/Compression Region
   C. Effect Of Length
   D. Effect Of The Foundation Stiffness
IV. Conclusions and Future Work
V. Acknowledgments and References

UNIVERSITY OF SOUTH CAROLINA

Introduction

A. Introduction To AFP
B. Tow Deformations Due To Steering

Introduction To AFP

UNIVERSITY OF SOUTH CAROLINA

- Automated Fiber Placement (AFP) is an **additive** process used to manufacture large composites **aerospace** structures.
- During the process, up to 32 **finite width** slit-tapes or tows are deposited by the machine head within a prescribed path.
- During the process, the layup **speed**, **temperature**, roller **compaction**, and **tow tension** are controlled to obtain a good layup quality.
- Tow **steering** is required to fabricate **curved** shells and **variable stiffness** plates.
- During the steering, the **straight** tows have to **deform** to adhere to the **curved path** on the tool surface.

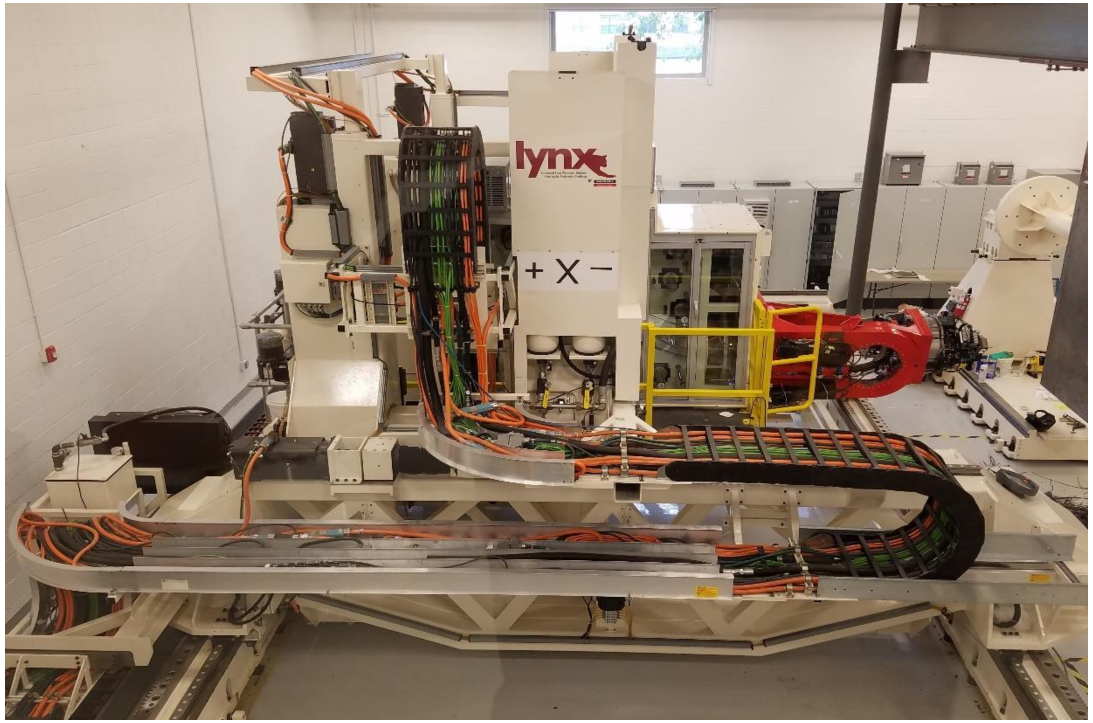

AFP machine at the McNair Center

Tow Deformations Due To Steering

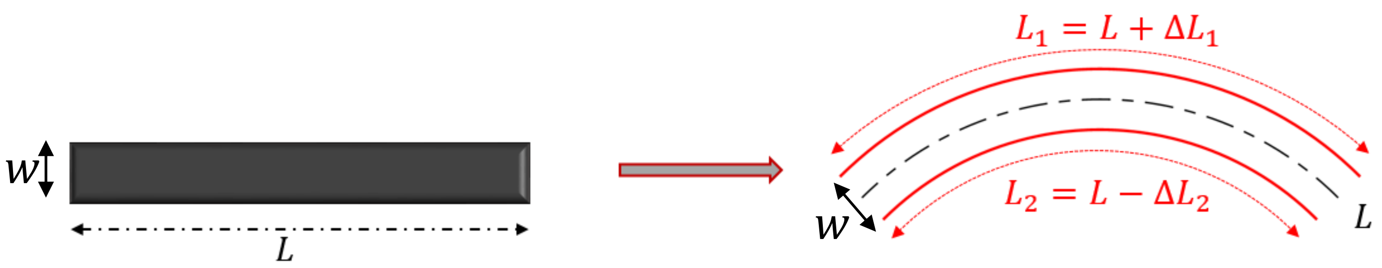

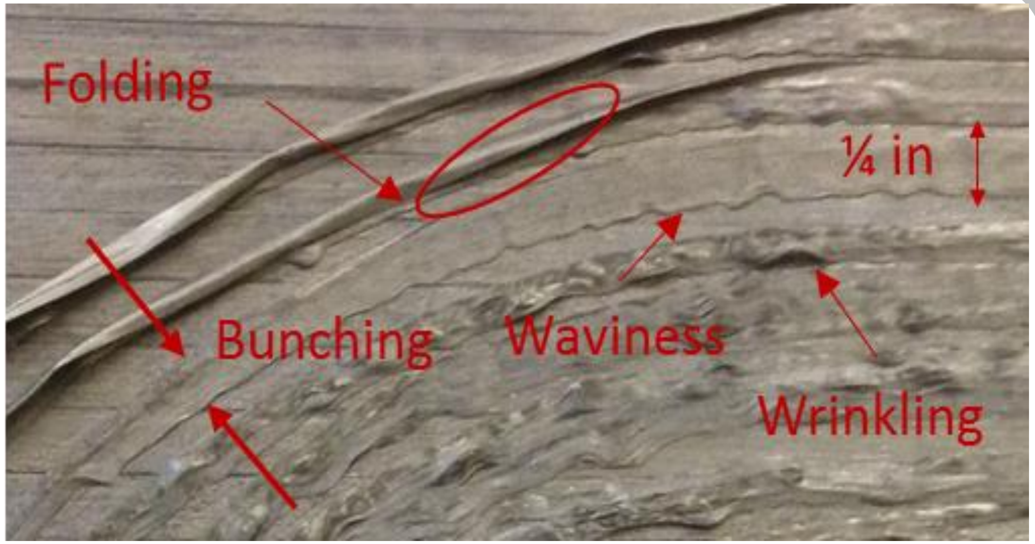

Possible deformation mechanisms

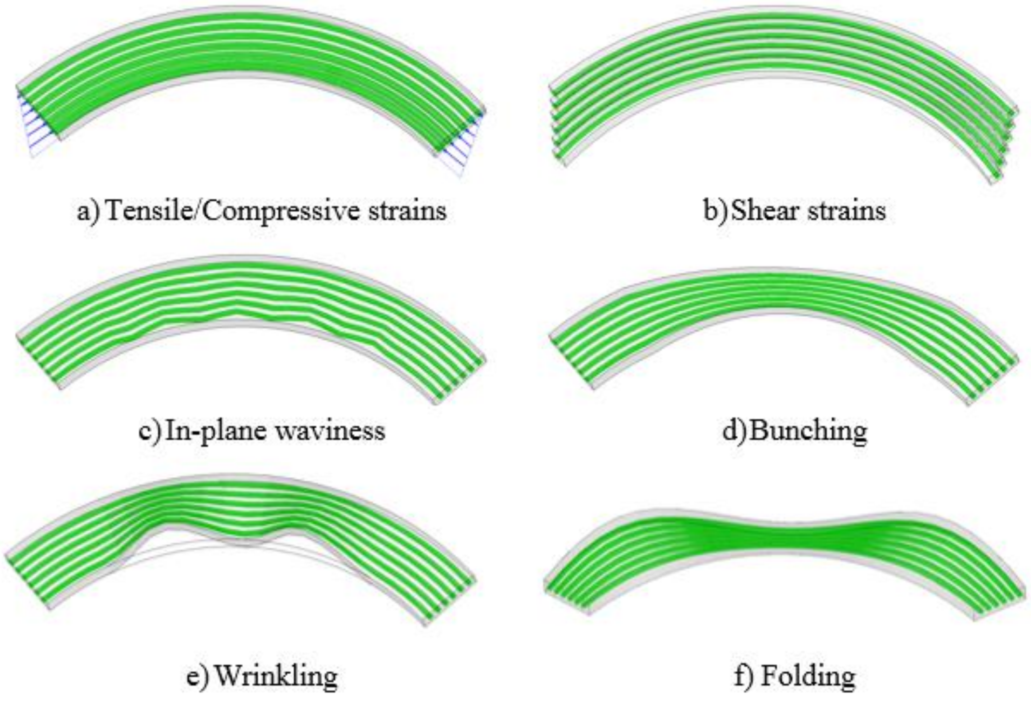

- Several deformation mechanisms are possible due to the mismatch of length between the tow and the prescribed path:
  - Elastic strain deformations
  - Large in-plane deformations
  - Large out-of-plane deformations
- The objective is to investigate the **tow deformations** with respect to the boundary conditions, material properties, and other process parameters.

Problem Formulation

A. Governing Equations
B. Numerical Solution Approach

Problem Formulation

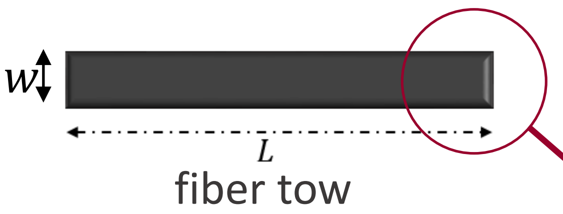

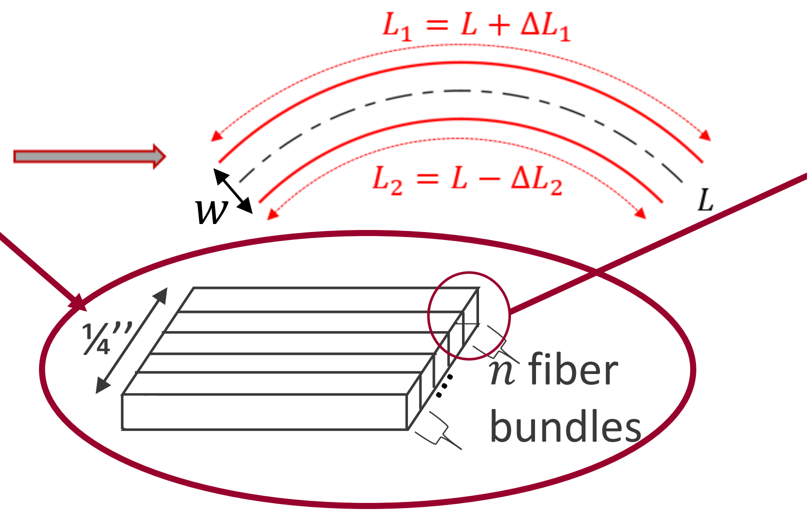

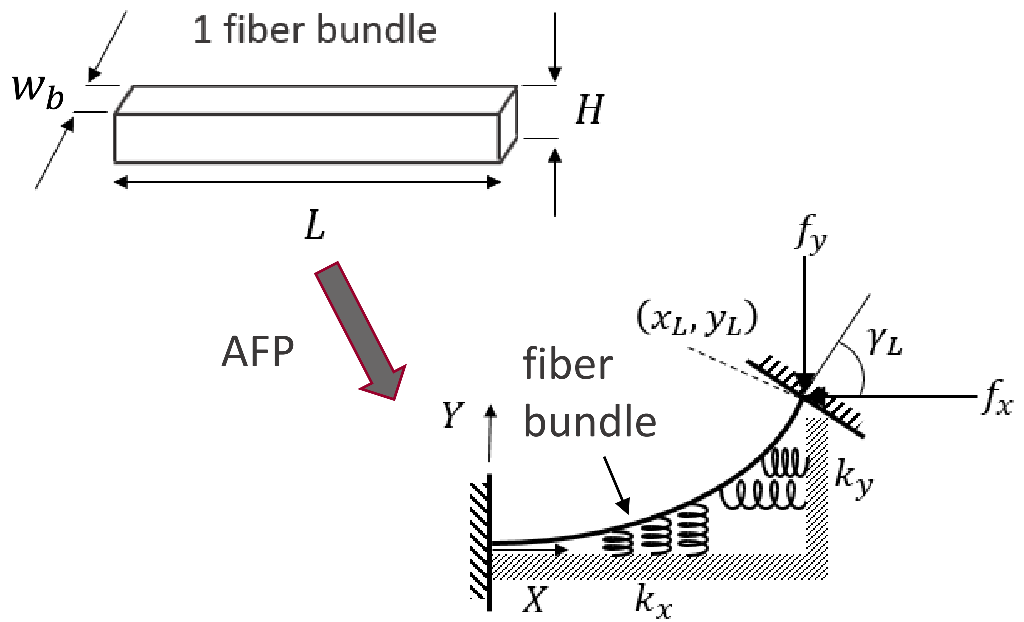

2D representation of a fiber bundle on stiff foundation

- Nomenclature:
  - γ, γ': in-plane rotation angle and in-plane curvature
  - β, β': out-of-plane rotation angle and curvature
  - l': axial strain
  - k_x, k_y, k_z: stiffness of the foundation (substrate) in the X, Y and Z directions
  - f_x, f_y, f_z: forces at the endpoint
  - u, v, w: displacements in the X, Y and Z directions
  - E_{11}: Elastic modulus in the fiber direction

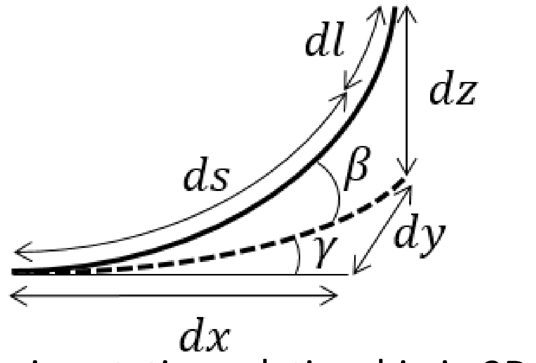

Strain-rotation relationship in 3D

Problem Formulation

Minimizing the total energy of the system, subject to the BCs constraints:

$$\Pi = U - W + K$$

Elastic Strain Energy — Work — Stored Energy

Elastic Strain Energy

$$U = \frac{1}{2}\int_0^L E_{11}\left(w_b H l' + I_\gamma \gamma'^2 + I_\beta \beta'^2\right) ds$$

Work

$$W = \boldsymbol{F}\cdot\boldsymbol{\Delta} \longrightarrow \boldsymbol{\Delta} = \{(x_L - x_0) - L, (y_L - y_0) - 0, (z_L - z_0) - 0\}$$

$$\boldsymbol{F} = \{f_x, f_y, f_z\}$$

$$W = f_x\left[\int_0^L (1 + l')\cos\gamma\cos\beta \; ds - L\right] + f_y\int_0^L (1 + l')\sin\gamma\cos\beta \; ds + f_z\int_0^L (1 + l')\sin\beta \, ds$$

Stored Energy

$$K = \frac{1}{2}\int_0^L k_x\, u^2(s)\, ds + \frac{1}{2}\int_0^L k_y\, v^2(s)\, ds + \frac{1}{2}\int_0^L k_z\, w^2(s)\, ds$$

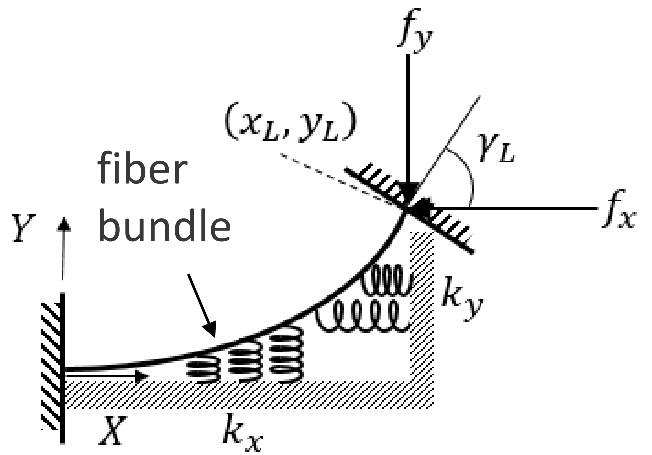

2D representation of a fiber bundle on stiff foundation

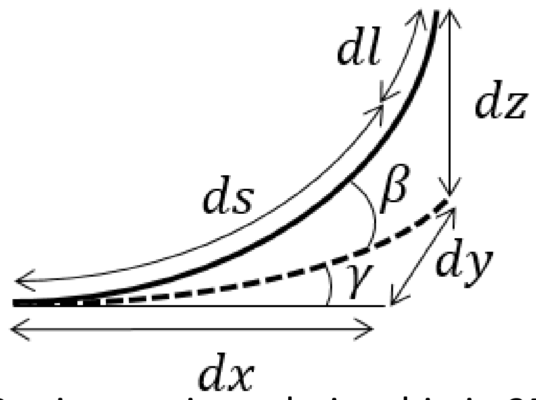

Strain-rotation relationship in 3D

Governing Equations

- Π is a functional of the form:

$$\Pi(\gamma(s),\beta(s),l(s)) = \int_0^L \mathcal{F}(s,\gamma(s),\gamma'(s),\beta(s),\beta'(s),l'(s))\,ds$$

- Euler-Lagrange equations to minimize the energy →

$$\begin{cases} \frac{d}{ds}\left(\frac{\partial \Pi}{\partial \gamma'}\right) - \frac{\partial \Pi}{\partial \gamma} = 0 \\ \frac{d}{ds}\left(\frac{\partial \Pi}{\partial \beta'}\right) - \frac{\partial \Pi}{\partial \beta} = 0 \\ \frac{d}{ds}\left(\frac{\partial \Pi}{\partial l'}\right) - \frac{\partial \Pi}{\partial l} = 0 \end{cases}$$

- Governing Equations:

Equilibrium:

$$\begin{cases} E_{11}I_\gamma\,\gamma'' - f_x \sin\gamma\cos\beta + f_y\cos\gamma\cos\beta + k_x u y - k_y v x = 0 \\ E_{11}I_\beta\,\beta'' - f_x\cos\gamma\sin\beta - f_y\sin\gamma\sin\beta + f_z\cos\beta + k_x u\xi + k_y v\psi - k_z w\zeta = 0 \\ E_{11}Al' = (F + f_x\cos\gamma\cos\beta + f_y\sin\gamma\cos\beta + f_z\sin\beta - k_x u x - k_y v y - k_z w z) \end{cases}$$

Geometry (strain-rotation relationships):

$$x' = (1+l')\cos\gamma\cos\beta$$
$$y' = (1+l')\sin\gamma\cos\beta$$
$$z' = (1+l')\sin\beta$$

Intermediate variables:

$$\xi' = (1+l')\cos\gamma\sin\beta$$
$$\psi' = (1+l')\sin\gamma\sin\beta$$
$$\zeta' = (1+l')\cos\beta$$

→ Unknowns

- functions: $\gamma(s)$, $\beta(s)$, $l'(s)$, $x(s)$, $y(s)$, $z(s)$, $\xi(s)$, $\psi(s)$, $\zeta(s)$
- Constants: f_x, f_y, f_z

- 14 BCs are needed to solve the system above:
  - Start point: @ $s = 0$: $\gamma(0) = \gamma_0, \beta(0) = \beta_0, l(0) = l_0, x(0) = x_0, y(0) = y_0, z(0) = z_0$ and $\xi(0) = \psi(0) = \zeta(0) = 0$
  - End point: @ $s = L$: $\gamma(L) = \gamma_L, \beta(L) = \beta_L, x(L) = x_L, y(L) = y_L, z(L) = z_L$

Numerical Solution Approach

UNIVERSITY OF SOUTH CAROLINA

- Introduce error function to satisfy the remaining 3 minimization constraints x_L, y_L and z_L:

$$\boldsymbol{G}(f_x, f_y, f_z) = \begin{Bmatrix} x^*(f_x, f_y, f_z) - x_L \\ y^*(f_x, f_y, f_z) - y_L \\ z^*(f_x, f_y, f_z) - z_L \end{Bmatrix} = \mathbf{0}$$

- x*, y* and z* are the solutions of the system @ s=L

- Use Newton-Raphson method for $G(f_x, f_y, f_z)$ iteratively to find the unknown forces:

$$\begin{Bmatrix} f_{x\,n+1} \\ f_{y\,n+1} \\ f_{z\,n+1} \end{Bmatrix} = \begin{Bmatrix} f_{x\,n} \\ f_{y\,n} \\ f_{z\,n} \end{Bmatrix} - c\, J^{-1}\left(f_{x\,n}, f_{y\,n}, f_{z\,n}\right)\, \boldsymbol{G}\left(f_{x\,n}, f_{y\,n}, f_{z\,n}\right)$$

- J is the Jacobian matrix for the vector **G**, and can be approximated using finite difference techniques

$$J = \left[\frac{\partial \boldsymbol{G}\left(f_{x\,n}, f_{y\,n}, f_{z\,n}\right)}{\partial f_x} \quad \frac{\partial \boldsymbol{G}\left(f_{x\,n}, f_{y\,n}, f_{z\,n}\right)}{\partial f_y} \quad \frac{\partial \boldsymbol{G}\left(f_{x\,n}, f_{y\,n}, f_{z\,n}\right)}{\partial f_y} \right]$$

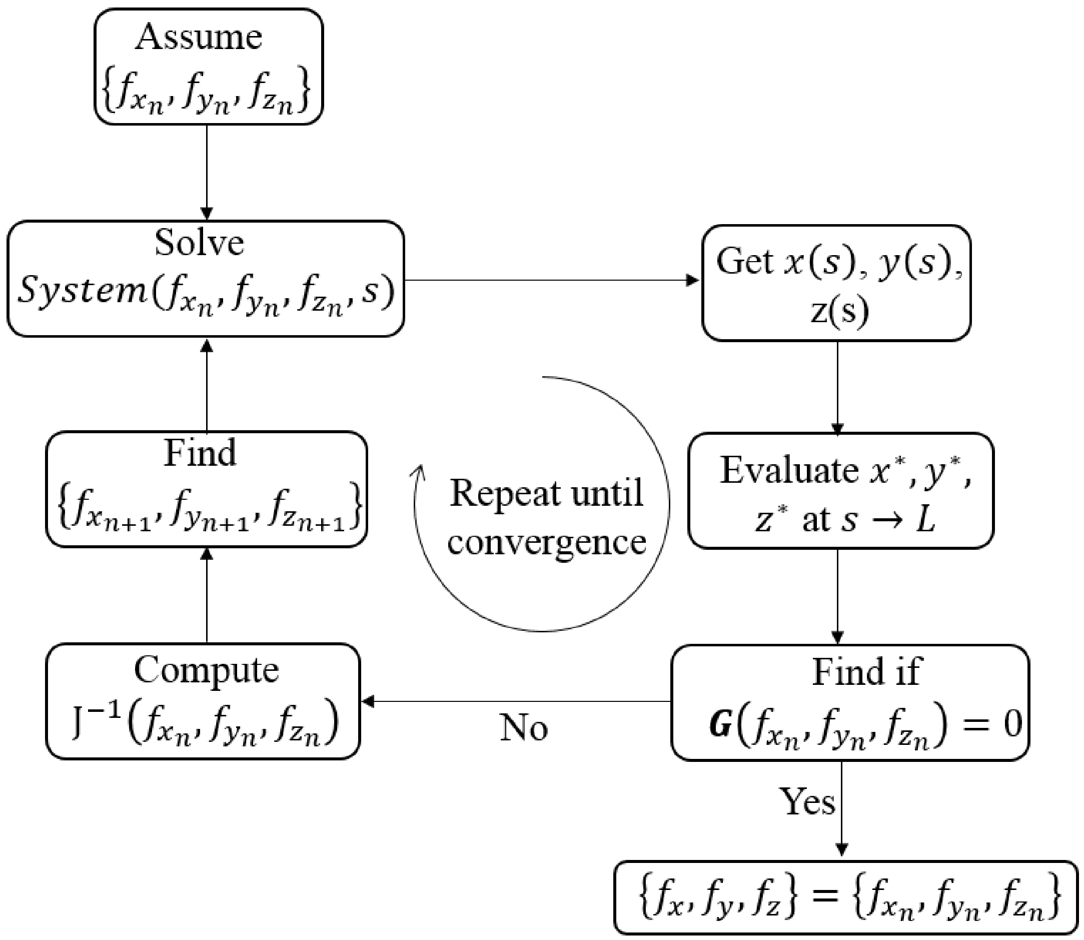

UNIVERSITY OF SOUTH CAROLINA

Results

A. Steering Boundary Conditions
B. Results For a Combined Tension/Compression Region
C. Effect Of Length
D. Effect Of The Foundation Stiffness

Steering Boundary Conditions

- For demonstration, A constant curvature tow-path is considered for analysis:

$$\boldsymbol{C}(s) = \{x(s), y(s), z(s)\} = \begin{cases} \rho \ \sin(s/\rho) \\ \rho[1 - \ \cos(s/\rho)] \ , \ \ 0 \le s \le L, \\ 0 \end{cases}$$

- The parallel edges of the tow-path are expressed as:

$$\boldsymbol{C_p}(s) = \{x_p(s), y_p(s), z_p(s)\} = \begin{cases} (d+\rho) \ \sin(s/\rho) \\ \rho - (d+\rho)\cos(s/\rho)] , \ \ 0 \le s \le L, \\ 0 \end{cases}$$

- The end-point BCs can be obtained from:

$$x_L = x_p(L), y_L = y_p(L) + d, z_L = 0, \gamma_L = \frac{L}{\rho}, \beta_L = 0.$$

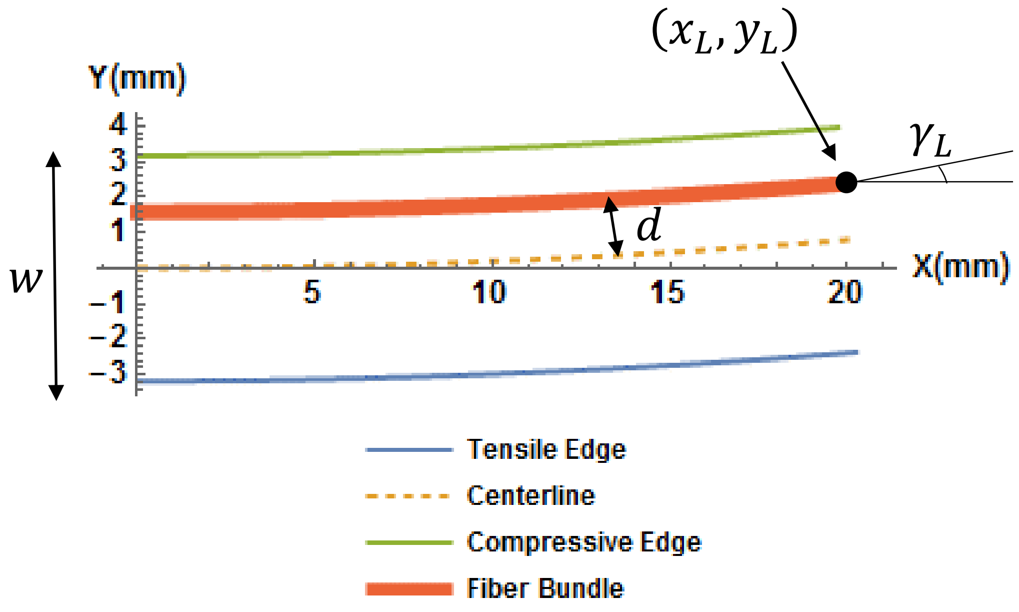

Constant curvature tow-path

Results For a Combined Tension/Compression Region

- Material Properties and tow geometry
  - $\rho = 0.8\,m$
  - $E_{11} = 130\,GPa$
  - $H = 0.184\,mm$
  - $\mathrm{w} = 6.35\,mm$
  - $k_x = k_y = k_z = 0$
  - $L = 40\,mm$

Deformed fiber bundles

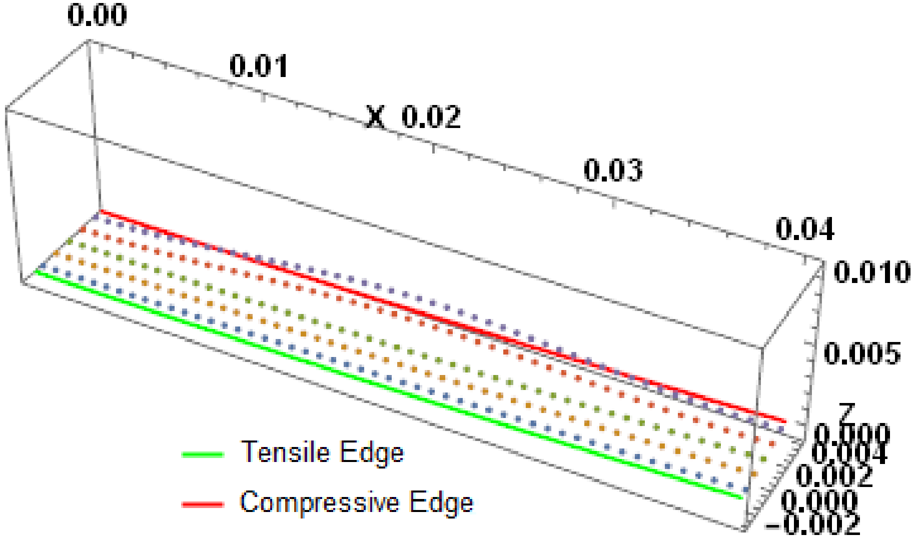

Cross-section at L/2

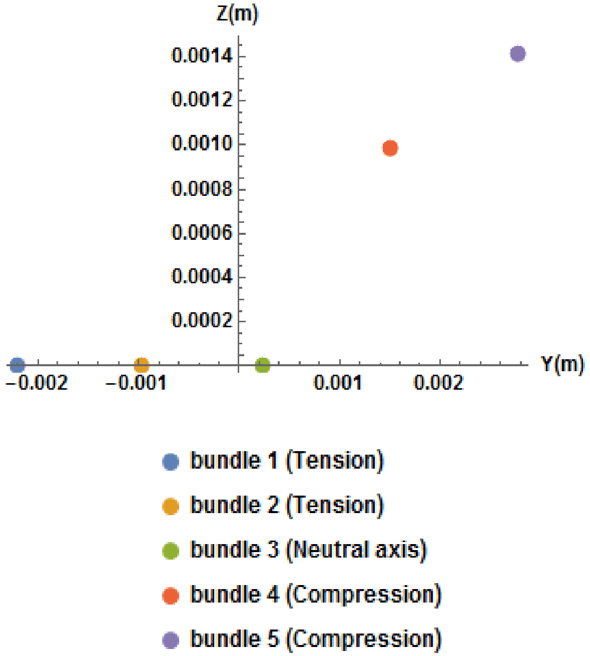

- Solution of the system (selected functions)

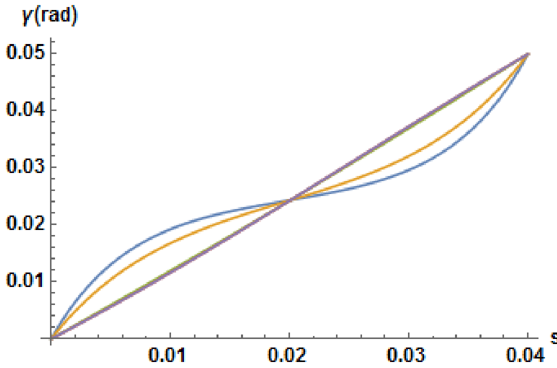

In-plane rotation

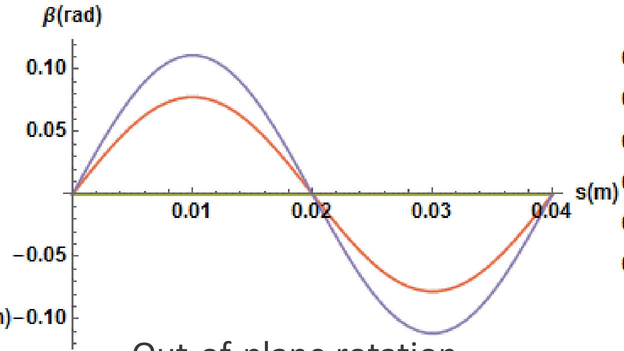

Out-of-plane rotation

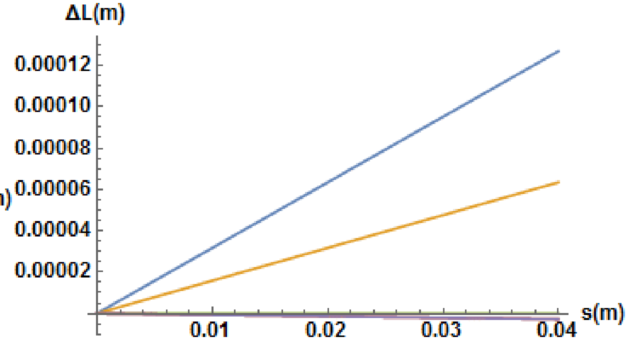

Strain along the length

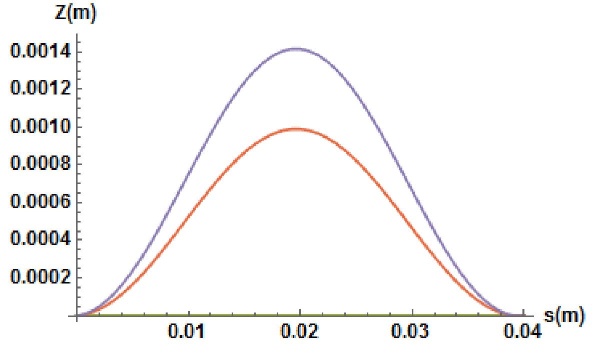

z-coordinate

Effect Of Length Under Compression

- Material Properties and tow geometry
  - $\rho = 0.8\ m$
  - $E_{11} = 130\ GPa$
  - $H = 0.184\ mm$
  - $\mathrm{w} = 6.35\ mm$
  - $k_x = k_y = k_z = 0$
  - L variable
- For short length:
  - Compressive strains are the main deformation mechanisms
- For large length:
  - Out-of-plane wrinkles start to occur

Deformed fiber bundles under compression at different length

$@\ L = 10\ mm$

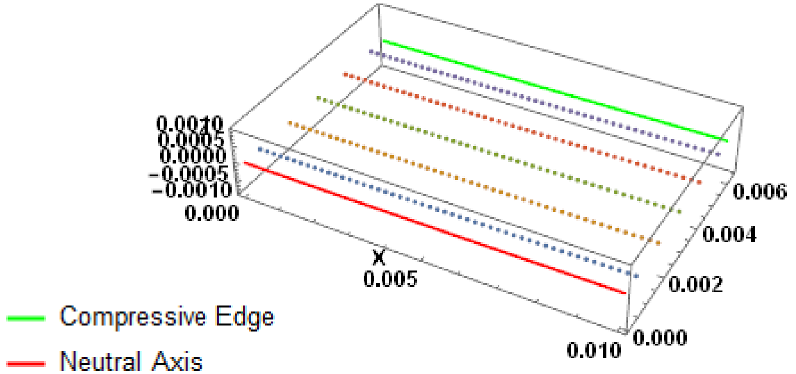

$@\ L = 20\ mm$

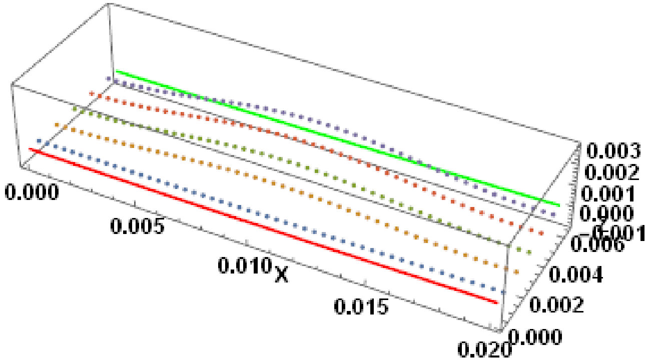

$@\ L = 40\ mm$

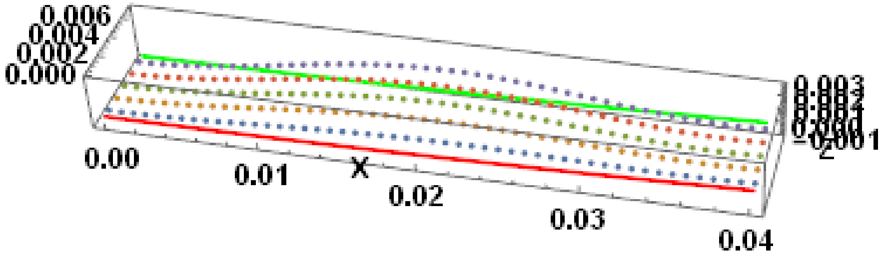

Effect Of The Foundation Stiffness

- Material Properties and tow geometry
  - $\rho = 0.8\ m$
  - $E_{11} = 130\ GPa$
  - $H = 0.184\ mm$
  - $\mathrm{w} = 6.35\ mm$
  - $k_x = k_y = k_z$: variable
  - $L = 2\ mm$
- For **large values** of k ($k > 10^6\ N/m^2$):
  - $w = 0$:The fiber bundles remain in their position as placed by the AFP head
- For **small values** of k ($k < 10^5\ N/m^2$):
  - Foundation is weak and the fibers wrinkle in the out-of-plane direction
- For $10^5 < k < 10^6\ N/m^2$:
  - Transition from wrinkles to strain deformations

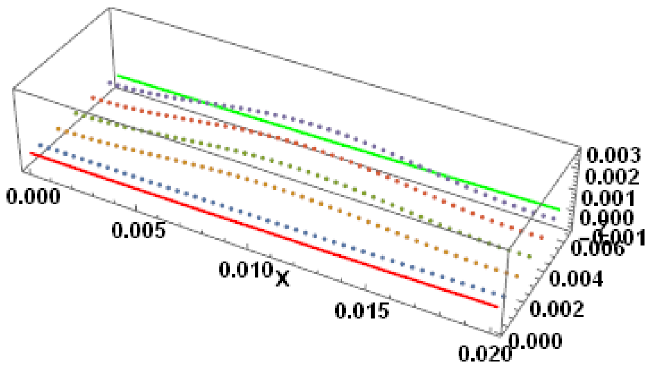

Deformed bundles for $k = 10^5\ N/m^2$

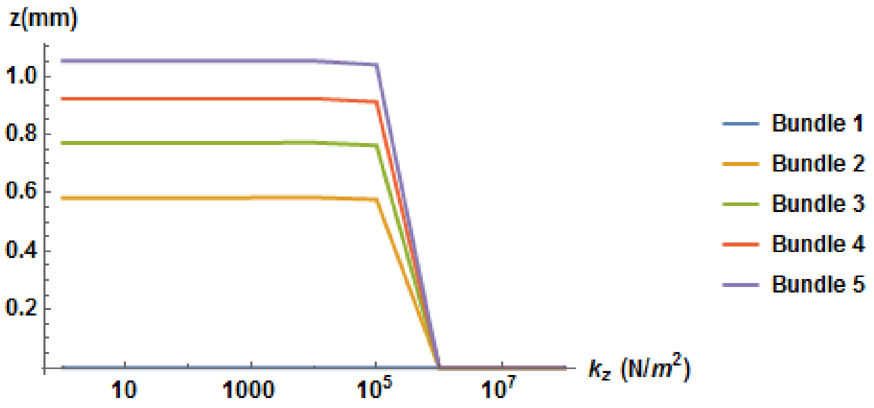

Effect of the foundation stiffness on the wrinkle formation

Conclusions & Future Work

Conclusions and Future Work

- The focus of this paper is to **understand** the formation of **tow deformations** during the AFP process.
- The tow is modeled as several **fiber bundles** laying on a **stiff foundation**.
- A **constant curvature** path is considered in the analysis where the results show that at a **small length** during the additive process, **strain** deformation are **dominant.**
- At **larger length**, **fiber wrinkling** occurs on the **compressive** side of the tow, whereas **fiber bunching/straightening** occurs on the **tensile** side of the tow.
- **Increasing** the **stiffness** of the foundation can **reduce** the out-of-plane deformation of the tow and possibly eliminating it for a very stiff foundation.

- Future work will consist of:
  - Investigating the **fiber bundles interaction** in the transverse direction through **shear** and **transverse** strains.
  - **Experimental** measurement of the **stiffness** of the foundation and relating it to other process parameters such as **speed** and layup **temperature**.
  - **Model validation** through comparison with steered tows manufactured using AFP.

Acknowledgement and References

- **Acknowledgments**:
  - The authors would like to thank The Boeing Company for their support of this work.

- **References**

G. Rousseau, R. Wehbe, J. Halbritter, and R. Harik, “Automated Fiber Placement Path Planning: A State-of-the-art review,” *Comput. Des. Appl.*, vol. 16, no. 2, pp. 172–203, 2019. doi:10.14733/cadaps.2019.172-203.

A. Sabido, L. Bahamonde, R. Harik, and M. J. L. Van Tooren, “Maturity assessment of the laminate variable stiffness design process,” *Compos. Struct.*, vol. 160, pp. 804–812, 2017. doi:10.1016/j.compstruct.2016.10.081.

R. Harik, C. Saidy, S. Williams, Z. Gurdal, and B. Grimsley, “Automated Fiber Placement Defect Identity Cards : Cause , Anticipation , Existence , Significance , and Progression,” in *SAMPE Conference & Exhibition*, 2018.

D. H. J. A. Lukaszewicz, C. Ward, and K. D. Potter, “The engineering aspects of automated prepreg layup: History, present and future,” *Compos. Part B Eng.*, vol. 43, no. 3, pp. 997–1009, 2012. doi:10.1016/j.compositesb.2011.12.003.

R. Wehbe, “Modeling of Tow Wrinkling in Automated Fiber Placement based on Geometrical Considerations,” University of South Carolina, 2017.

R. Y. Wehbe, R. Harik, and Z. Gurdal, “In-plane tow deformations due to steering in automated fiber placement,” in *AIAA Scitech 2019 Forum*, American Institute of Aeronautics and Astronautics, 2019. doi:10.2514/6.2019-1271.

S. Rajan, M. A. Sutton, R. Wehbe, B. Tatting, Z. Gürdal, and A. Kidane, “Experimental investigation of prepreg slit tape wrinkling during automated fiber placement process using StereoDIC,” *Compos. Part B*, vol. 160, no. December 2018, pp. 546–557, 2019. doi:10.1016/j.compositesb.2018.12.017.

A. Beakou, M. Cano, J. B. Le Cam, and V. Verney, “Modelling slit tape buckling during automated prepreg manufacturing: A local approach,” *Compos. Struct.*, vol. 93, no. 10, pp. 2628–2635, 2011. doi:10.1016/j.compstruct.2011.04.030.

M. Y. Matveev, P. J. Schubel, A. C. Long, and I. A. Jones, “Understanding the buckling behaviour of steered tows in Automated Dry Fibre Placement (ADFP),” *Compos. Part A Appl. Sci. Manuf.*, vol. 90, pp. 451–456, 2016. doi:10.1016/j.compositesa.2016.08.014.

R. Wehbe, B. F. Tatting, R. Harik, Z. Gürdal, A. Halbritter, and S. Wanthal, “TOW-PATH BASED MODELING OF WRINKLING DURING THE AUTOMATED FIBER PLACEMENT PROCESS,” *Compos. Adv. Mater. Expo CAMX2017*, 2017.

P. M. Hormann, *Thermoset automated fibre placement - on steering effects and their prediction*. 2015.